Ultrafast Photoinduced Electron Transfer in Directly Linked Porphyrin−Ferrocene Dyads

Minoru Kubo,*,†,‡ Yukie Mori,§ Masana Otani,† Masataka Murakami,† Yukihide Ishibashi,† Masakazu Yasuda,† Kohei Hosomizu,|| Hiroshi Miyasaka,† Hiroshi Imahori,*,§,|| and Satoru Nakashima*,†

Department of Materials Engineering Science, Graduate School of Engineering Science, Osaka University, Toyonaka 560-8531, Japan, Fukui Institute for Fundamental Chemistry, Kyoto University, Kyoto 606-8103, Japan, and Department of Molecular Engineering, Graduate School of Engineering, Kyoto University, Kyoto 615-8510, Japan

Received: February 24, 2007; In Final Form: April 17, 2007

The ultrafast electron transfer occurring upon Soret excitation of three new porphyrin−ferrocene (XP−Fc) dyads has been studied by femtosecond up-conversion and pump−probe techniques. In the XP−Fc dyads (XP−Fcs) designed in this study, the ferrocene moiety is covalently bonded to the meso positions of 3,5-di-*tert*-butylphenyl zinc porphyrin (BPZnP−Fc), pentafluorophenyl zinc porphyrin (FPZnP−Fc), and 3,5-di-*tert*-butylphenyl free-base porphyrin (BPH_2P−Fc). Charge separation and recombination in the XP−Fcs were confirmed by transient absorption spectra, and the lifetimes of the charge-separated states were estimated from the decay rate of the porphyrin radical anion band to be approximately 20 ps. The charge-separation rates of the XP−Fcs were found to be $>10^{13}$ s^{-1} from the S_2 state and 6.3×10^{12} s^{-1} from the S_1 state. Charge separation from the S_2 state was particularly efficient for BPZnP−Fc, whereas the main reaction pathway was from the S_1 state for BPH_2P−Fc. Charge separation from the S_2 and S_1 states occurred at virtually the same rate in benzene and tetrahydrofuran and was much faster than their solvation times. Analysis of these results using semiquantum Marcus theory indicates that the magnitude of the electronic-tunneling matrix element is rather large and far outside the range of nonadiabatic approximation. The pump−probe data show the presence of vibrational coherence during the reactions, suggesting that wavepacket dynamics on the adiabatic potential energy surface might regulate the ultrafast reactions.

Introduction

The kinetics and dynamics of electron-transfer (ET) reactions are fundamental issues in fields ranging from physical chemistry to biology, and the theory of ET reactions in condensed media has been developed on the basis of Marcus theory.[1−9] According to this theory, the ET rate is determined by the donor−acceptor electronic coupling, the free-energy gap, and the reorganization energies of the medium and the intramolecular vibrations. Apart from these energy parameters, the ET rate is also regulated by dynamic parameters such as the relaxation times of solvent polarization and intramolecular vibrations. To date, Marcus theory has been applied to a wide range of ET reactions.[10−12]

On the other hand, with recent progress in femtosecond spectroscopy, research attention has shifted toward ET reactions that are faster than diffusive solvation dynamics and/or vibrational relaxation.[13−19] We previously reported an example of such an ET reaction in a porphyrin−ferrocene dyad with a pentafluorophenyl free-base porphyrin directly linked to ferrocene (abbreviated as FPH_2P−Fc; FP = pentafluorophenyl, H_2P = free-base porphyrin, Fc = ferrocene).[20] After Soret excitation of this system, rapid ET occurs from the S_1 state with a time constant of 110 fs after S_2−S_1 internal conversion (IC) in both tetrahydrofuran (THF) and benzene. ET from the S_2 state is not observed in this system because of the rapid IC.

In the present study, the photodynamics in other types of porphyrin−ferrocene dyads was studied with femtosecond up-conversion (UC) and pump−probe (PP) techniques. We designed three porphyrin−ferrocene (XP−FC) dyads: BPZnP−Fc (BP = 3,5-di-*tert*-butylphenyl, ZnP = zinc porphyrin), FPZnP−Fc, and BPH_2P−Fc (Figure 1), which are denoted hereafter as XP−Fcs. The differences between these XP−Fcs are the presence of either electron-donating (BP) or electron-withdrawing (FP) substituents and metal (Zn) or metal-free (H_2) centers in the porphyrin component. In this article, we discuss the ultrafast ET from both the S_2 state and the S_1 state that occurs in these XP−Fc systems. ET from the S_2 state was found to occur in under 100 fs and to be most efficient in BPZnP−Fc. The femtosecond UC and PP data demonstrate that the rates of ET from the S_2 and S_1 states are higher than those of the solvent relaxation processes and are independent of the solvent polarity and the free-energy gap. The PP data also indicate the presence of vibrational coherence during the reactions. On the basis of these results and the analysis with semiquantum Marcus theory, possible reaction mechanisms are discussed for the ultrafast ET occurring in the XP−Fc systems.

Experimental Section

Synthesis. Pyrrole, trifluoroacetic acid, Et_3N, and ferrocenecarboxyaldehyde were purchased from Kanto Chemicals (Tokyo, Japan). $Zn(OAc)_2 \cdot 2H_2O$ and *p*-chloranil were purchased from Nacalai Tesque (Kyoto, Japan). All solvents were obtained

* Corresponding authors. E-mail: M.Kubo@neu.edu (M.K.), satoru@chem.es.osaka-u.ac.jp (S.N.), imahori@scl.kyoto-u.ac.jp (H.I.).
† Osaka University.
‡ Present address: Department of Physics, Northeastern University, Boston, Massachusetts 02115.
§ Fukui Institute for Fundamental Chemistry, Kyoto University.
|| Graduate School of Engineering, Kyoto University.

10.1021/jp071546b CCC: $37.00
Published on Web 05/27/2007

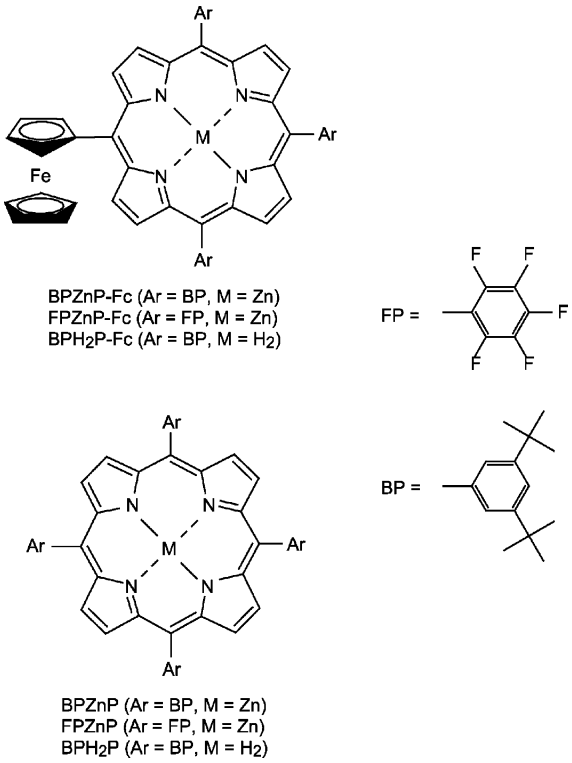

Figure 1. Structural formulas of the three XP−Fcs and their reference XPs.

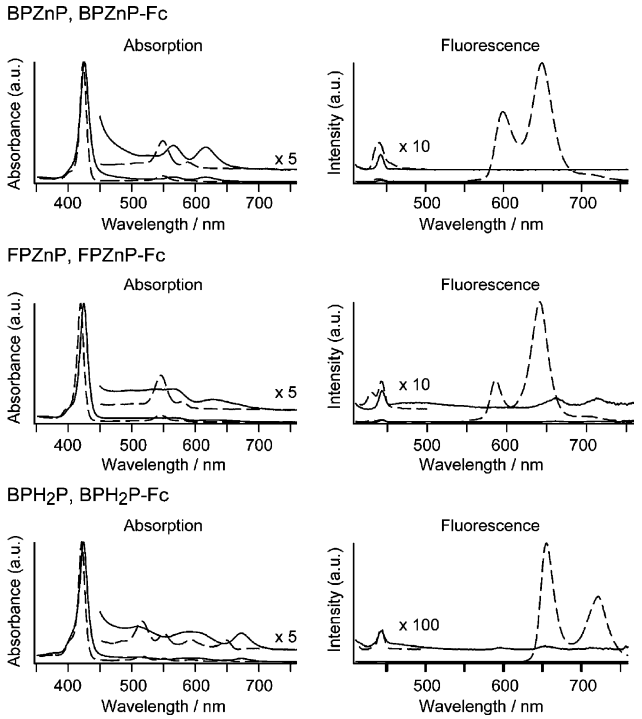

Figure 2. Steady-state absorption and fluorescence (excited at 390 nm) spectra in benzene. The spectra of the XP−Fcs and XPs are shown in solid and dashed lines, respectively. Enlarged traces multiplied by the indicated factors are also shown.

from Wako Pure Chemical Industries Ltd. (Osaka, Japan) and were used without further purification. ^{1}H NMR spectra were recorded on an EX-400 spectrometer (JEOL, Tokyo, Japan). Matrix-assisted laser desorption/ionization (MALDI) mass spectra (MS) were measured on a KOMPACT MALDI II instrument (Shimadzu Corporation, Kyoto, Japan).

XP−Fcs were synthesized by procedures reported for similar A_3B-type meso-substituted porphyrins, i.e., by acid-catalyzed condensation of 2-formylferrocene, 3,5-di-*tert*-butylbenzaldehyde (or pentafluorobenzaldehyde), and pyrrole, followed by oxidation with chloranil.[21] Flash column chromatography of the reaction mixture on neutral silica gel (Kanto Chemicals, silica gel 60N, spherical) with hexane/dichloromethane as the eluent gave the desired dyads as the second eluted bands. Zinc was inserted by addition of an excess of zinc acetate in a mixture of $CHCl_3$ and methanol. Reference XPs were prepared according to the method in the literature.[21]

BPH_2P−Fc. Pyrrole (268 mg, 4 mmol), ferrocenecarboxyaldehyde (429 mg, 2 mmol), and 3,5-di-*tert*-butylbenzaldehyde (437 mg, 2 mmol) were dissolved in 200 mL of $CHCl_3$. Trifluoroacetic acid (0.3 mL) was then injected through a syringe under Ar, and the resulting mixture was stirred for 2 h at room temperature. To the reaction mixture was added *p*-chloranil (740 mg, 3 mmol), and the mixture was stirred at room temperature overnight. The reaction was then quenched with Et_3N (0.75 g, 7.4 mmol), and the solvent was removed in vacuo. The residue was purified by flash column chromatography over SiO_2 eluted with CH_2Cl_2 to yield BPH_2P−Fc (45 mg, 0.042 mmol, 4.2%) as a purple-red solid. ^{1}H NMR ($CDCl_3$, 400 MHz) δ 10.00 (2H, s), 8.78−8.81 (6H, m), 8.07 (4H, s), 7.79 (2H, s), 7.76 (1H, s), 5.59 (2H, s), 4.84 (2H, s), 4.22 (5H, s), 1.54 (36H, s), 1.51 (18H, s), −2.26 (2H, s). MS (MALDI-TOF) m/z = 1060 (M + H^+).

BPZnP−Fc. BPH_2P−Fc (53 mg, 50 μmol) was dissolved in $CHCl_3$ (15 mL), and saturated $Zn(OAc)_2 \cdot 2H_2O$ in MeOH (0.6 mL) was added through a syringe. The resulting mixture was stirred for 3 h under Ar at 60 °C. After being cooled, the mixture was washed with distilled water and brine. The organic phase was then dried over $MgSO_4$, and the solvent was removed in vacuo. The residue was purified by flash column chromatography over SiO_2 eluted with hexane/CH_2Cl_2 (2/1−1/1) to yield BPZnP−Fc (32 mg, 28 μmol, 56%) as a purple solid. ^{1}H NMR ($CDCl_3$, 400 MHz) δ 10.23 (2H, d, J = 4.8 Hz), 8.94 (2H, d, J = 4.8 Hz), 8.90−8.93 (4H, ABq), 8.08 (4H, d, J = 1.6 Hz), 8.05 (2H, d, J = 1.6 Hz), 7.79 (2H, t, J = 1.6 Hz), 7.76 (1H, t, J = 1.6 Hz), 5.58 (2H, s), 4.83 (2H, s), 4.29 (5H, s), 1.55 (37H, s), 1.54 (18H, s). MS (MALDI-TOF) m/z = 1122 (M + H^+).

FPH_2P−Fc. Pyrrole (403 mg, 6 mmol), ferrocenecarboxyaldehyde (642 mg, 3 mmol), and pentafluorobenzaldehyde (588 mg, 3 mmol) were dissolved in 300 mL of $CHCl_3$. Trifluoroacetic acid (0.47 mL) was then injected through a syringe under Ar, and the resulting mixture was stirred for 2 h at room temperature. To the reaction mixture was added *p*-chloranil (1.23 g, 5 mmol), and the mixture was stirred at room temperature overnight. The reaction was quenched with Et_3N (1.0 g, 9.9 mmol), and the solvent was removed in vacuo. The residue was purified by flash column chromatography over SiO_2 eluted with CH_2Cl_2/hexane (1/2−1/1) to yield FPH_2P−Fc (65 mg, 0.065 mmol, 4.3%) as a purple solid. ^{1}H NMR ($CDCl_3$, 400 MHz) δ 10.12 (2H, d, J = 4.5 Hz), 8.77 (4H, s), 8.74 (2H, d, J = 4.5 Hz), 5.59 (2H, s), 4.92 (2H, s), 4.23 (5H, s), −2.28 (2H). MS (MALDI-TOF) m/z = 993 (M + H^+).

FPZnP−Fc. FPH_2P−Fc (35 mg, 35 μmol) was dissolved in $CHCl_3$ (5 mL), and saturated $Zn(OAc)_2 \cdot 2H_2O$ in MeOH (0.5 mL) was added to the mixture through a syringe. The resulting mixture was refluxed for 3 h under Ar. After being cooled, the mixture was washed with distilled water and brine. The organic phase was dried over $MgSO_4$, and the solvent was removed in vacuo. The residue was purified by flash column chromatography over SiO_2 eluted with hexane/CH_2Cl_2 (2/1−1/1) to yield FPZnP−Fc (25 mg, 0.028 mmol, 70%) as a purple solid. ^{1}H

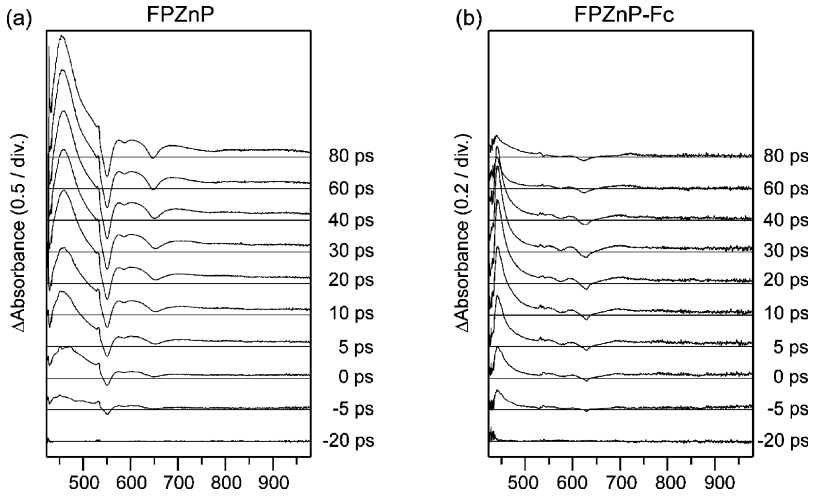

Figure 3. Transient absorption spectra of FPZnP and FPZnP−Fc in THF after excitation with a 532-nm laser pulse with a fwhm of 15 ps.

NMR ($CDCl_3$, 400 MHz) δ 10.30 (2H, d, J = 4.8 Hz), 8.87 (4H, s), 8.83 (2H, d, J = 4.8 Hz), 5.56 (2H, s), 4.88 (2H, s), 4.21 (5H, s). MS (MALDI-TOF) m/z = 1055 ($M + H^+$).

Cyclic Voltammetry. Cyclic voltammograms were obtained using a 0.1 M *n*-Bu_4NPF_6 solution in N_2-saturated THF with a scan rate of 0.05 V s^{-1} on a CH Instruments model 660 A electrochemical workstation at room temperature. Glassy carbon, Pt wire, and Ag/Ag^+ (0.01 M $AgNO_3$, 0.1 M *n*-Bu_4NClO_4 in MeCN) electrodes were used as the working, counter, and reference electrodes, respectively. Ferrocene was used as the internal standard.

Spectroscopy. The details of the UC measurements were described previously.[22] The cross-correlation trace between the fundamental and its second harmonic pulses gave ≤50 fs fwhm (full width at half-maximum) at the sample position. The time-resolved S_2 fluorescence excited at 390 nm was monitored at 440 nm, whereas the time-resolved S_1 fluorescence excited at 410 nm was monitored at 650 nm for BPZnP, 627 nm for BPZnP−Fc, and 642 nm for the other compounds.

In the single-color PP measurements, the output of the second harmonics of a homemade cavity-dumped Ti:sapphire laser at 200-kHz repetition rate, centered at 424 nm with a 15-nm bandwidth, was divided into pump and probe beams.[20] The fwhm of the autocorrelation trace at the sample position was ∼35 fs. In the two-color PP measurements, on the other hand, a dual OPA femtosecond laser system[23] was employed, in which the wavelengths of the pump and probe beams were set to 400 and 705 nm, respectively. The fwhm of the cross-correlation trace between the pump and probe pulses was 170 fs at the sample position. Transient absorption spectra were obtained using a 532-nm excitation pulse with 15-ps fwhm and a white-light continuum probe pulse with the PP system described previously.[24]

Results

Steady-State Absorption and Fluorescence Spectra. The absorption spectra of the XPs and XP−Fcs are shown in Figure 2. The Soret bands of the XP−Fcs were found to be similar to those of the reference XPs, although the peak for each XP−Fc is slightly red-shifted with respect to and broader than that for each XP. In contrast, the Q bands of the XP−Fcs are significantly different in shape and position from those of the XPs. The fluorescence spectra of the XPs and XP−Fcs are also shown in Figure 2. Very weak S_2 fluorescence was observed for the XPs and XP−Fcs. The intensities of the S_2 fluorescence peaks of the XP−Fcs relative to those of the XPs were roughly 60%, 70%, and 90% for BPZnP−Fc, FPZnP−Fc, and BPH_2P−Fc, respectively. The S_1 fluorescence of the XP−Fcs was quenched more dramatically. The S_1 fluorescence intensities of the XP−Fcs were only <5% of those of the XPs. In particular, the S_1 fluorescence of BPZnP−Fc was found to be completely quenched (<0.5%). These results for S_2 and S_1 fluorescence quenching suggest the involvement of ET reaction pathways from the S_2 and S_1 states.

Subpicosecond−Picosecond Transient Absorption Changes. To directly probe the ET reactions, transient absorption spectroscopy was applied to FPZnP and FPZnP−Fc in THF. Figure 3a shows the transient absorption spectra of FPZnP excited with a 532-nm laser pulse with a fwhm of 15 ps. The spectra are characterized by a strong absorption band at 457 nm and dip signals corresponding to the bleaching of the Q bands at 550 and 586 nm, which are ascribed to the S_1-S_n transition. The bleaching at 648 nm might be due to the induced emission from the S_1 state. In contrast to the spectra of FPZnP, the spectra of FPZnP−Fc contain characteristic bands of the porphyrin radical anion, including a strong, sharp band around 450 nm ($\epsilon \approx 10^5$ M^{-1} cm^{-1}) and weak, broad bands in the range 700−900 nm ($\epsilon \approx 10^4$ M^{-1} cm^{-1}) (Figure 3b).[25] The ferrocenium cation band near 800 nm could not be distinguished because of its small molar extinction coefficient ($\epsilon \approx 10^3$ M^{-1} cm^{-1}). The porphyrin radical anion bands, which emerge within the apparatus response function, decay as a result of charge recombination (CR) on a time scale of several tens of picoseconds.

To elucidate the dynamic behavior of the ET process for shorter times, the time profile of the transient absorbance at 705 nm was measured after Soret excitation at 400 nm, using laser pulses with a fwhm of 170 fs (Figure 4). An ultrafast rise of the transient absorbance within the apparatus response function is followed by a rapid decay with a time constant of approximately 0.2 ps (0.18−0.25 ps). The ultrafast rise might involve S_2-S_1 IC and charge separation (CS) from the S_2 state. The subsequent rapid decay is due to CS from the S_1 state, because this time constant is comparable to the S_1 fluorescence lifetime (vide infra). Note that the decay absorbance change due to CS from the S_1 state implies that the extinction coefficient of the S_1 state at 705 nm is larger than that of the charge-separated state. Following this subpicosecond decay, a slight rise occurs with a time constant of approximately 6 ps (4.0−6.7 ps), and then there is a decay with a time constant of approximately 20 ps (22−25 ps). The slow decay stems from

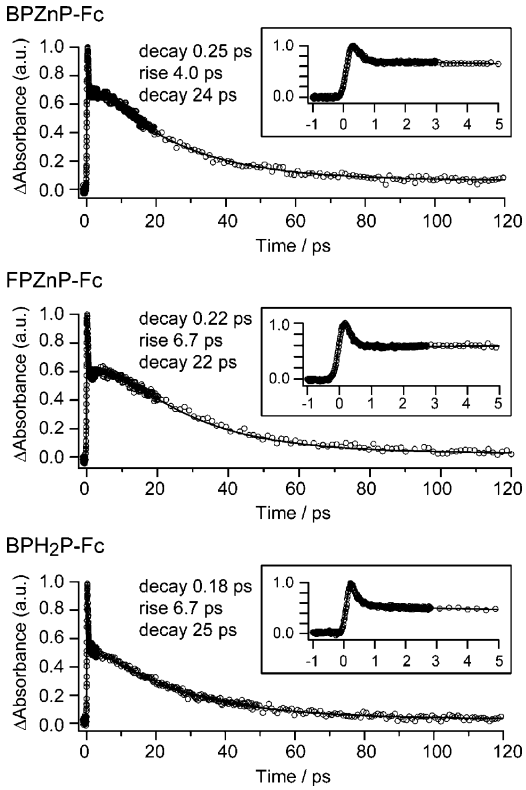

Figure 4. Absorbance changes at 705 nm in THF after excitation at 400 nm. The changes in the early-time region are shown in the inset. Observed signals (circles) were fitted with exponential functions (solid lines). The apparatus response function was taken into account.

CR as shown in Figure 3, whereas the picosecond rise might be due to vibrational cooling and/or structural relaxation in the charge-separated state.

Time Profiles of the S_2 and S_1 Fluorescence. The S_2 and S_1 fluorescence decays of the XPs and XP−Fcs were measured in benzene using the UC method with an apparatus response function of ≤50 fs. The S_2 fluorescence decays of the XP−Fcs were found to be very rapid, with time constants of ≤80 fs, and are appreciably faster than those of the corresponding reference XPs, particularly for BPZnP−Fc. This result strongly suggests that rapid CS from the S_2 state occurs in competition with the S_2−S_1 IC. The S_1 fluorescence decays of the XP−Fcs were also found to be rapid, with a time constant of approximately 160 fs, which is consistent with the extremely weak intensity of the S_1 fluorescence in the steady-state measurements (Figure 2). The rapid decay of the S_1 fluorescence results from CS from the S_1 state, as is evident in Figures 3 and 4. Time-resolved fluorescence emission could not be detected in THF because of the strong Raman scattering from THF.[26]

PP Measurements in the Femtosecond Time Region. To shed light on the early dynamics after Soret excitation, transient absorption changes were measured at 424 nm using the PP technique with a higher time resolution of 35 fs. The transient absorption spectra (Figure 3) feature absorptions at 424 nm in the S_1 state of the XPs and in the charge-separated states of the XP−Fcs. Thus, the S_1 state absorption and the charge-separated state absorption as well as the ground-state bleaching contribute to the present PP signals. Figure 6 below shows the PP signals of the XPs and XP−Fcs in THF and benzene. The time constants of the dynamics are very similar in THF and benzene, and are in agreement with the data for fluorescence in benzene displayed in Figure 5.

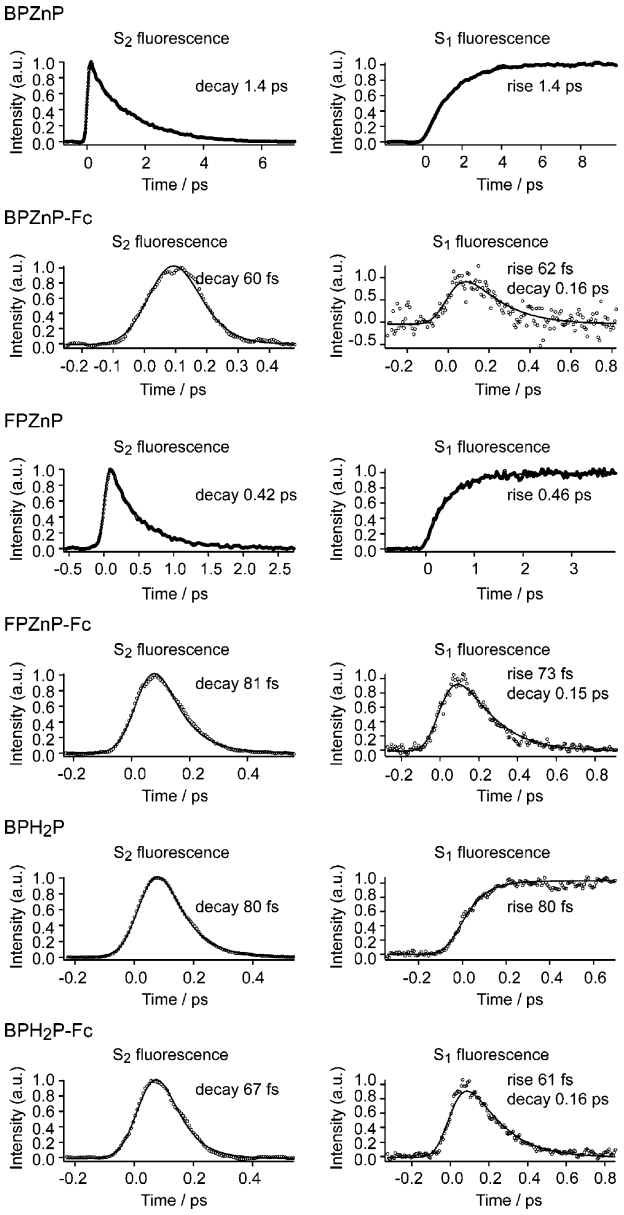

Figure 5. UC signals in benzene. Observed signals (circles) were fitted with exponential functions (solid lines). The apparatus response function was taken into account.

The signal of BPZnP consists of two components with subpico- and picosecond time constants (see the top panel of Figure 6). The slow component (1.2−1.5 ps) is assigned to S_2−S_1 IC, as this time constant is in agreement with the S_2 fluorescence lifetime. The fast component (0.38−0.39 ps) cannot be assigned unambiguously as yet, but might involve a relaxation process in the S_2 state. The signal of FPZnP also results from subpicosecond and picosecond dynamics. The fast component (0.39−0.48 ps) matches the S_2 fluorescence lifetime and is assigned to S_2−S_1 IC, whereas the slow component (2.7−3.7 ps) is due to a relaxation process in the S_1 state. Similarly, the signal of BPH_2P consists of ultrafast S_2−S_1 IC (80−87 fs) and a picosecond relaxation in the S_1 state (2.6−2.8 ps).

On the other hand, the dynamics of all of the XP−Fcs feature an ultrafast rise with a time constant of ∼60−70 fs, followed by a decay with a time constant of ∼160 fs and a slow decay on the picosecond time scale. By comparing these time constants with those in Figures 3−5, we attribute the first two components to the population dynamics of the S_2 and S_1 states, respectively.

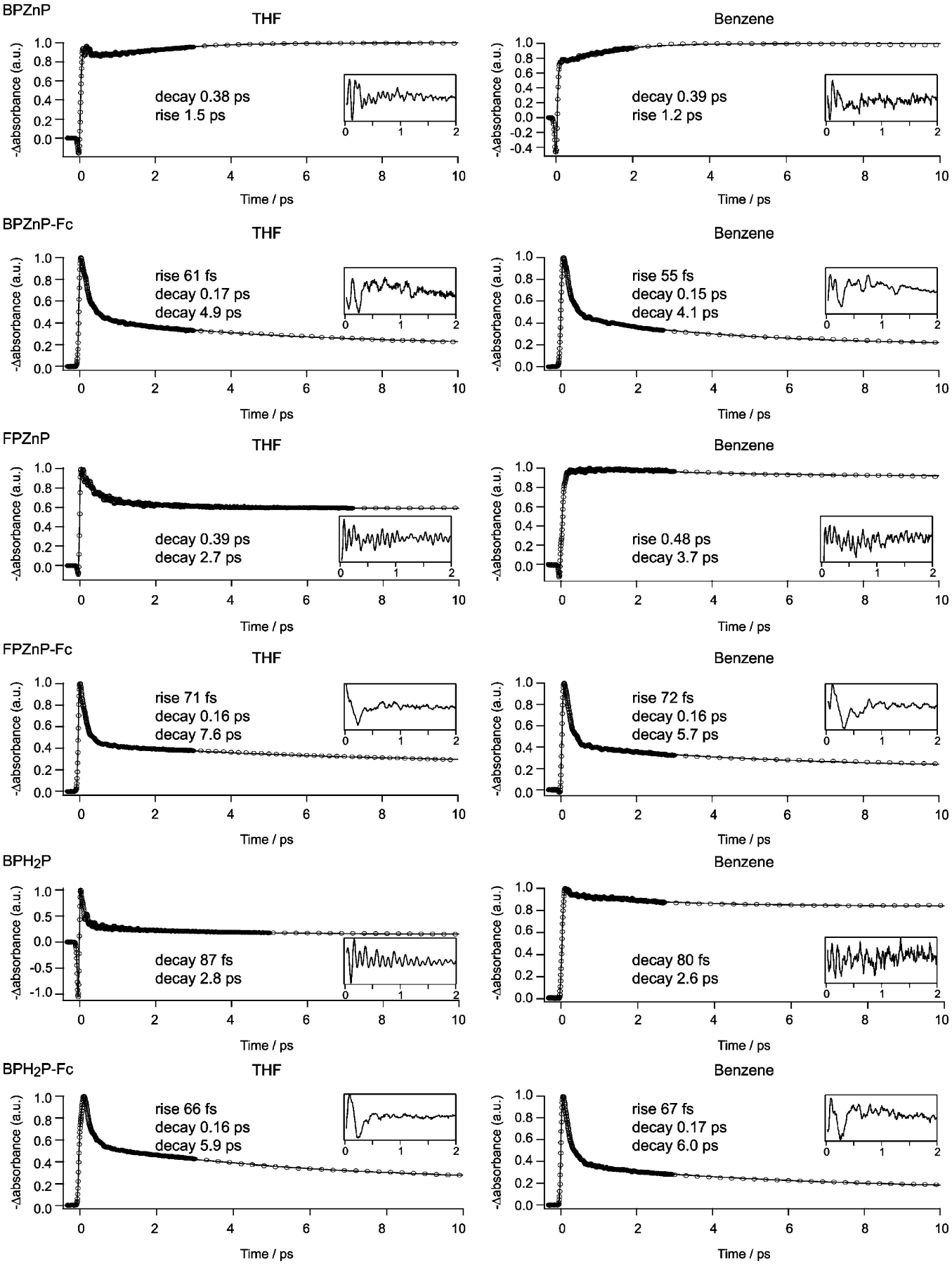

Figure 6. PP signals at 424 nm in THF and benzene. Observed signals (circles) were fitted with exponential functions (solid lines). The apparatus response function was taken into account. The coherent spikes were fitted with a Gaussian and an exponential rise. The insets show the oscillatory components obtained by subtracting the fitted population components from the PP signals.

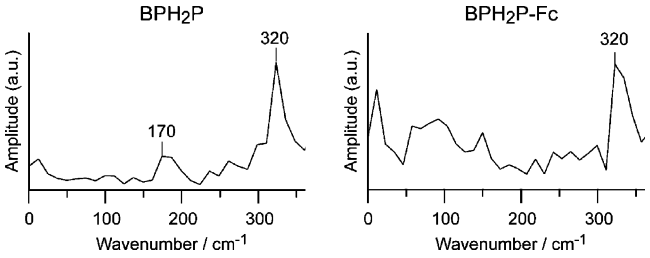

Figure 7. Fourier-transform frequency spectra of BPH_2P and BPH_2P−Fc in benzene. The effect of the pulse width was corrected.

TABLE 1: ET Rates and Free-Energy Gaps of the XP−Fcs in THF

	BZnP−Fc	FPZnP−Fc	BPH_2P−Fc	FPH_2P−Fc[a]
$\tau_{CS}(S_2)$ (fs)	63	89	–	–
$\tau_{CS}(S_1)$ (fs)	160	160	160	110
τ_{CR} (ps)	24	22	25	no data
λ_S (eV)	0.79	0.79	0.79	0.79
$E_{ox} - E_{red}$ (eV)	1.97	1.52	1.75	1.52
ΔG_S (eV)	−0.29	−0.29	−0.29	−0.29
$-\Delta G_{CR}$ (eV)	1.68	1.23	1.46	1.23
$\Delta E(S_2)$ (eV)	2.86	2.87	2.88	2.89
$\Delta E(S_1)$ (eV)	1.95	1.93	1.80	1.79
$-\Delta G_{CS}(S_2)$ (eV)	1.18	1.64	1.42	1.66
$-\Delta G_{CS}(S_1)$ (eV)	0.27	0.70	0.34	0.56

[a] Data for FPH_2P−Fc were obtained from ref 20.

The picosecond component is probably due to structural relaxation in the charge-separated state.

In addition to the ultrafast dynamic behavior, vibrational coherence results in oscillatory modulation of the PP signals of the XPs and the XP−Fcs (see the insets in Figure 6). Fourier-transform frequency spectra of the oscillation data for BPH_2P and BPH_2P−Fc in benzene are shown in Figure 7. The most intense peak in both spectra is at 320 cm^{-1}, which is assigned to the porphyrin-ring breathing mode (ν_8).[27] The second strongest peak in the spectrum of BPH_2P is at 170 cm^{-1}, which arises from the phenyl translation mode (ϕ_{10}).[27] For BPH_2P−Fc, on the other hand, the signal-to-noise level did not allow us to determine lower-frequency peaks. Pronounced vibrational coherence was observed for FPH_2P−Fc at frequencies of 130, 200, 250, and 330 cm^{-1} with a better signal-to-noise ratio; the detailed analysis of this coherence has been reported elsewhere.[20]

Rates and Free-Energy Gaps of the CS reactions. The rate of CS from the S_2 state [$k_{CS}(S_2) = \tau_{CS}(S_2)^{-1}$] can be roughly estimated with the equation $\tau_{CS}(S_2)^{-1} = \tau_{XP-Fc}(S_2)^{-1} - \tau_{XP}(S_2)^{-1}$, where $\tau_{XP-Fc}(S_n)$ and $\tau_{XP}(S_n)$ are the S_n-state lifetimes of the XP−Fc and the XP, respectively. However, we note that $\tau_{CS}(S_2)$ of BPH_2P−Fc cannot be estimated because the $\tau_{XP-Fc}(S_2)$ and $\tau_{XP}(S_2)$ values in this system are very similar. The rate of CS from the S_1 state [$k_{CS}(S_1) = \tau_{CS}(S_1)^{-1}$] can be well approximated as $\tau_{XP-Fc}(S_1)^{-1}$ because $\tau_{XP}(S_1)^{-1}$ is orders of magnitude smaller. The $\tau_{CS}(S_2)$ and $\tau_{CS}(S_1)$ values of the XP−Fcs in THF are summarized in Table 1. The CS rates in benzene could not be distinguished from those in THF on the basis of the UC and PP data.

The free-energy gap for CS ($-\Delta G_{CS}$) can be estimated using the following equations[28]

$$-\Delta G_{CS}(S_n) = \Delta E(S_n) - (-\Delta G_{CR}) \quad (1)$$

$$-\Delta G_{CR} = E_{ox} - E_{red} + \Delta G_S \quad (2)$$

$$\Delta G_S = e^2[1/(2R_D) + 1/(2R_A)](1/\epsilon_s - 1/\epsilon_r) - e^2/(\epsilon_s R_{DA}) \quad (3)$$

Here, $\Delta E(S_n)$ is the excitation energy of the S_n state; $-\Delta G_{CR}$ is the free-energy gap for CR; and E_{ox} and E_{red} are the first oxidation and first reduction potentials, respectively. ΔG_S is the correction term that includes the effects of the solvent and the Coulombic interaction between the charged donor and acceptor. The third equation for ΔG_S is known as the Born equation.[29] R_D and R_A are the radii of the charged donor and acceptor, respectively, and R_{DA} is the center-to-center distance between them. ϵ_r is the dielectric constant of the solvent in which E_{ox} and E_{red} are determined (THF), and ϵ_s is that of the solvent used in the spectroscopic measurements (THF or benzene). The Born equation is appropriate for polar solvents such as THF and has yielded satisfactory results in many cases.[1b,12,30] However, for less polar or almost nonpolar solvents (e.g., benzene), ΔG_S is often overestimated with this equation under the continuum approximation. The estimation of the solvent reorganization energy λ_s also has a similar problem

$$\lambda_s = e^2[1/(2R_D) + 1/(2R_A) - 1/R_{DA}](1/\epsilon_\infty - 1/\epsilon_s) \quad (4)$$

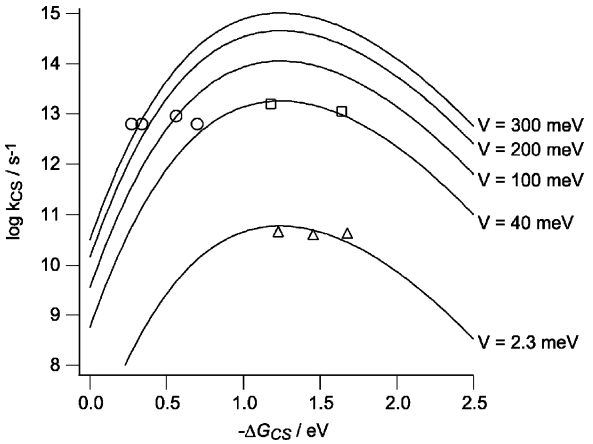

Figure 8. Semilogarithmic energy gaps for $k_{CS}(S_1)$ (○), $k_{CS}(S_2)$ (□), and k_{CR} (△) in THF. The curves were calculated with semiquantum Marcus theory for $V = 2.3$, 40, 100, 200, and 300 meV. $T = 298$ K, $\lambda_v = 0.5$ eV, $\hbar\langle\omega\rangle = 0.15$ eV, $\lambda_s = 0.79$ eV ($R_A = 10$ Å, $R_D = 2$ Å, and $R_{DA} = 6.5$ Å).

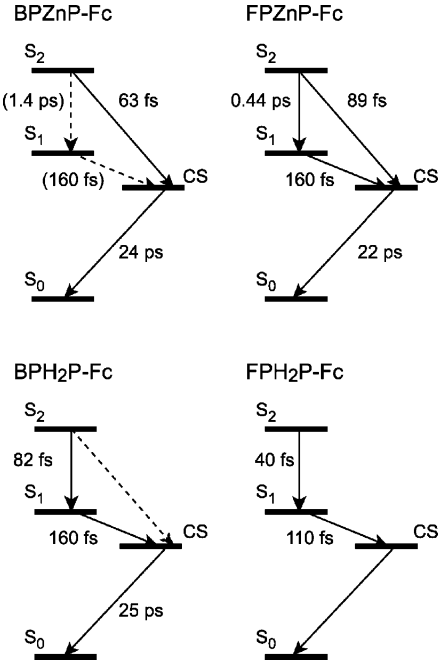

Figure 9. Reaction scheme after Soret excitation of the XP−Fcs. The primary and secondary reaction pathways are shown as solid and dashed arrows, respectively. The data for FPH_2P−Fc were obtained from ref 20.

The λ_s value for benzene calculated with eq 4 is negligibly small because the optical dielectric constant ϵ_∞ is very similar to the static dielectric constant ϵ_s. Thus, we estimated $-\Delta G_{CS}$ of the XP−Fcs in THF (Table 1) and plotted the CS rates against $-\Delta G_{CS}$ in THF (Figure 8).

The relationship between k_{CS} and ΔG_{CS} was analyzed with the semiquantum Marcus expression

$$k_{CS} = (2\pi/\hbar)V^2(4\pi\lambda_s k_B T)^{-1/2}\sum_n[e^{-S}(S^n/n!)]\exp[-(\Delta G_{CS} + \lambda_s + n\hbar\langle\omega\rangle)^2/4\lambda_s k_B T] \quad (5)$$

where V is the donor−acceptor electronic-tunneling matrix element, $S = \lambda_v/\hbar\langle\omega\rangle$ is the electron−vibration coupling constant, and λ_v is the reorganization energy associated with the average angular frequency $\langle\omega\rangle$ of the intramolecular high-frequency vibrations. Marcus theory is well applicable to directly linked donor−acceptor systems despite the short donor−acceptor separation compared to their molecular sizes, as confirmed for porphyrin−imide dyads.[30b−d] We found that fitting the ultrafast CS rates to the Marcus parabola required $V > 40$ meV, for an adiabaticity parameter[4] of $\kappa_A > 1$. This indicates that the CS reactions in the XP−Fcs are adiabatic. On the other hand, the plots for the CR rates were placed on the $V = 2.3$ meV curve in the nonadiabatic region, which is comparable to the results obtained for other porphyrin-linked systems.[30a,31]

Discussion

The present time-resolved spectroscopy reveals the ultrafast ET reactions following Soret excitation of the XP−Fcs. The relatively long lifetime of the S_2 state of ZnP enabled us to investigate the ET reaction pathways from the S_2 state as well as from the S_1 state. The time constant for ET from the S_2 state was as high as ∼60 fs, which is comparable to the highest time constant ever reported for intermolecular ET in condensed media.[15,16,19b]

Because the S_0-S_2 excitation energy of porphyrin (∼2.9 eV) is very close to the S_0-S_1 excitation energy of ferrocene (∼2.8 eV),[32,33] energy transfer from porphyrin to ferrocene is an alternative explanation for the ultrashort S_2 lifetimes of the XP−Fcs. However, based on the Förster dipole−dipole model,[34] the energy-transfer rate is estimated to be $<3.7 \times 10^{11}$ s^{-1} for BPZnP−Fc. Here, because there are no structural data for the orientation of ferrocene relative to the porphyrin plane, the maximum possible value of the orientation factor (κ) was used to estimate the upper limit of the rate constant [$\langle\kappa\rangle^2 \le (4/\pi)^2$ when Jablonski's two-dimensional transition dipole moment is assumed for ZnP].[35] The low rate constant of energy transfer is due to the small extinction coefficient of ferrocene (<96 M^{-1} cm^{-1})[33] and the small S_2 fluorescence quantum yield of porphyrin (3.7×10^{-4} for ZnTPP).[36] It should be noted that, when the distance between donor and acceptor is short compared to their molecular sizes, the dipole−dipole model is not accurate because of the contribution of dipole−quadrupole interaction;[37] however, it is still useful for an order-of-magnitude estimation of energy-transfer rate, which was confirmed for porphyrin−fullerene dyads.[38] The S_2 fluorescence quenching of BPZnP−Fc is two orders of magnitude faster than the estimated upper limit of energy-transfer rate. Hence, energy transfer by the Förster Coulombic mechanism is ruled out.

Energy transfer by the Dexter electron-exchange mechanism[37] is also ruled out. The oxidation potential E_{ox} of BPZnP was found to be ∼0.4 eV (vs Fc/Fc$^+$ in THF), indicating that the energy level of the highest occupied molecular orbital (HOMO) of porphyrin is lower than that of ferrocene. The oxidation potential of porphyrin in the S_2 state is also lower than that of ferrocene in the S_1 state because the excitation energies are nearly the same. Thus, ferrocene cannot accept the excited electron from porphyrin via Dexter-type electron exchange, although electron transfer does occur from the HOMO of ferrocene to the HOMO of excited porphyrin, as observed in the present study.

It is worth mentioning that, in some donor−bridge−acceptor systems, the acceptor containing iron d electrons was found to enhance intersystem crossing of the donor, depending on the coordination and spin states of the iron.[39] In the XP−Fcs, however, no apparent role of spin−orbit coupling was found in the ultrafast processes. Actually, there is no triplet-state signal in the transient absorption spectra.

The reaction scheme for the series of XP−Fcs including FPH_2P−Fc[20] is summarized in Figure 9. ET from the S_2 state is the most efficient for BPZnP−Fc, whereas ET mainly occurs in BPH_2P−Fc from the S_1 state after the rapid S_2-S_1 IC. FPZnP−Fc is an intermediate case between BPZnP−Fc and BPH_2P−Fc, i.e., both pathways from the S_2 and S_1 states are effective for ET.

The energy-gap dependences of the CR rates of the XP−Fcs are not obvious because the CR rates occur near the top region of the Marcus parabola (Figure 8), which indicates that the CR processes are almost barrierless. It should be noted that the inclusion of the effect of intramolecular high-frequency vibrations ($\hbar\langle\omega\rangle = 0.15$ eV, $\lambda_v = 0.5$ eV) is essential to reproduce the observed CR rates. This means that the reaction is facilitated by quantum-mechanical vibrational channels.

On the other hand, the ultrahigh CS rates cannot be explained solely in terms of the effect of the intramolecular high-frequency vibrations. Ultrafast ET on the subpicosecond time scale in porphyrin−imide dyads has previously been successfully interpreted using semiquantum Marcus theory with $\hbar\langle\omega\rangle = 0.15$ eV, $\lambda_v = 0.3$ eV, and the electronic-tunneling matrix element $V \approx 20$ meV.[30b−d] Because this V value is the upper limit of the nonadiabatic approximation,[28] the ET in these systems still obeys semiquantum Marcus theory. On the other hand, the V value for ET from both the S_2 and S_1 states in the XP−Fcs has to be 40 meV or higher to achieve the observed ET rates. This magnitude of V is far outside the range of semiquantum Marcus theory under the nonadiabatic approximation. Moreover, the ET from the S_2 and S_1 states of the XP−Fcs is insensitive to the solvent polarity and much faster than the initial solvation time (0.43 ps for THF and 0.53 ps for benzene).[40] These results demonstrate that the solvent dynamics are not the driving force for ET in the XP−Fcs.

The single-color PP data show that there is vibrational coherence during the ET reactions (Figure 6), which indicates that the reactions proceed under nonequilibrium conditions before vibrational relaxation is completed. In a previous study,[20] we demonstrated that ultrafast ET in FPH_2P−Fc is controlled by translational and rotational motions of the ferrocene moiety relative to the porphyrin plane in the coherent regime, which modulate the π-orbital overlap between porphyrin and ferrocene to achieve the adiabatic electronic coupling. This coherent reaction mechanism might be common in the XP−Fcs. However, the vibrational coherence presented here is much more complicated than that in FPH_2P−Fc, because of the involvement of the wavepacket motions in the S_2 state as well as in the S_1 state, the charge-separated state, and the ground state. Quantum-dynamical simulations of the wavepacket motion in the excited states[41,42] are needed to determine the role of vibrational coherence in the ultrafast ET in the XP−Fcs.

In summary, we have designed three porphyrin−ferrocene dyads with different substituents and different centers in the porphyrin component. The variation in these systems of the S_2−S_1 IC rates has a large impact in determining whether the main reaction pathway of ET is from the S_2 or S_1 state. The ET processes in these systems were found to be ultrafast and independent of the solvation dynamics and free-energy gap. A vibrationally coherent reaction mechanism on the adiabatic potential surface would be plausible for the ultrafast photoinduced ET in the directly linked donor−acceptor systems.

Acknowledgment. This work was partially supported by a Grant-in-Aid for the JSPS Fellowship for Young Scientists to M.K. This work was also supported by Grants-in-Aid [Molecular Nano Dynamics (432) to H.M. and 21st Century COE on Kyoto University Alliance for Chemistry to H.I.] from the Ministry of Education, Culture, Sports, Science and Technology (MEXT), Japan.

References and Notes

(1) (a) Marcus, R. A. *J. Chem. Phys.* **1956**, *24*, 966−978. (b) Marcus, R. A.; Sutin, N. *Biochim. Biophys. Acta* **1985**, *811*, 265−322.

(2) Zusman, L. D. *Chem. Phys.* **1980**, *49*, 295−304.

(3) Calef, D. F.; Wolynes, P. G. *J. Phys. Chem.* **1983**, *87*, 3387−3400.

(4) Rips, I.; Jortner, J. *J. Chem. Phys.* **1987**, *87*, 2090−2104.

(5) Hynes, J. T. *J. Phys. Chem.* **1986**, *90*, 3701−3706.

(6) Jortner, J.; Bixon, M. *J. Chem. Phys.* **1988**, *88*, 167−170.

(7) Bagchi, B.; Gayathri, N. *Adv. Chem. Phys.* **1999**, *107*, 1−80.

(8) (a) Sumi, H.; Marcus, R. A. *J. Chem. Phys.* **1986**, *84*, 4894−4914. (b) Nadler, W.; Marcus, R. A. *J. Chem. Phys.* **1987**, *86*, 3906−3924.

(9) (a) Walker, G. C.; Akesson, E.; Johnson, A. E.; Levinger, N. E.; Barbara, P. F. *J. Phys. Chem.* **1992**, *96*, 3728−3736. (b) Barbara, P. F.; Walker, G. C.; Smith, T. P. *Science* **1992**, *256*, 975−981. (c) Kliner, D. A. V.; Tominaga, K.; Walker, G. C.; Barbara, P. F. *J. Am. Chem. Soc.* **1992**, *114*, 8323−8325. (d) Tominaga, K.; Kliner, D. A. V.; Johonson, A. E.; Levinger, N. E.; Barbara, P. F. *J. Chem. Phys.* **1993**, *98*, 1228−1243.

(10) Wasielewski, M. R. *Chem. Rev.* **1992**, *92*, 435−461.

(11) Bixon, M.; Jortner, J. *Adv. Chem. Phys.* **1999**, *106*, 35−202.

(12) Mataga, N.; Miyasaka, H. *Adv. Chem. Phys.* **1999**, *107*, 431−496.

(13) (a) Vos, M. H.; Lambry, J. C.; Robles, S. J.; Youvan, D. C.; Breton, J.; Martin, J.-L. *Proc. Natl. Acad. Sci. U.S.A.* **1991**, *88*, 8885−8889. (b) Vos, M. H.; Rappaport, F.; Lambry, J.-C.; Breton, J.; Martin, J.-L. *Nature* **1993**, *363*, 320−325.

(14) Wynne, K.; Reid, G. D.; Hochstrasser, R. M. *J. Chem. Phys.* **1996**, *105*, 2287−2297.

(15) (a) Seel, M.; Engleitner, S.; Zinth, W. *Chem. Phys. Lett.* **1997**, *275*, 363−369. (b) Engleitner, S.; Seel, M.; Zinth, W. *J. Phys. Chem. A* **1999**, *103*, 3013−3019. (c) Baigar, E.; Gilch, P.; Zinth, W.; Stöckl, M.; Härter, P.; von Feilitzsch, T.; Michel-Beyerle, M. E. *Chem. Phys. Lett.* **2002**, *352*, 176−184.

(16) (a) Yoshihara, K.; Tominaga, K.; Nagasawa, Y. *Bull. Chem. Soc. Jpn.* **1995**, *68*, 696−712. (b) Rubtsov, I. V.; Shirota, H.; Yoshihara, K. *J. Phys. Chem. A* **1999**, *103*, 1801−1808. (c) Rubtsov, I. V.; Yoshihara, K. *J. Phys. Chem. A* **1999**, *103*, 10202−10212.

(17) (a) Fiebig, T.; Stock, K.; Lochbrunner, S.; Riedle, E. *Chem. Phys. Lett.* **2001**, *345*, 81−88. (b) Pandurski, E.; Fiebig, T. *Chem. Phys. Lett.* **2002**, *357*, 272−278.

(18) Nakashima, S.; Nagasawa, Y.; Seike, K.; Okada, T.; Sato, M.; Kohzuma, T. *Chem. Phys. Lett.* **2000**, *331*, 396−402.

(19) (a) Kambhampati, P.; Son, D. H.; Kee, T. W.; Barbara, P. F. *J. Phys. Chem. A* **2000**, *104*, 10637−10644. (b) Son, D. H.; Kambhampati, P.; Kee, T. W.; Barbara, P. F. *J. Phys. Chem. A* **2002**, *106*, 4591−4597.

(20) Kubo, M.; Mori, Y.; Otani, M.; Murakami, M.; Ishibashi, Y.; Yasuda, M.; Hosomizu, K.; Miyasaka, H.; Imahori, H.; Nakashima, S. *Chem. Phys. Lett.* **2006**, *429*, 91−96.

(21) (a) Tkachenko, N. V.; Lemmetyinen, H.; Sonoda, J.; Ohkubo, K.; Sato, T.; Imahori, H.; Fukuzumi, S. *J. Phys. Chem. A* **2003**, *107*, 8834−8844. (b) Kashiwagi, Y.; Imahori, H.; Araki, Y.; Ito, O.; Yamada, K.; Sakata, Y.; Fukuzumi, S. *J. Phys. Chem. A* **2003**, *107*, 5515−5522.

(22) Bhasikuttan, A. C.; Suzuki, M.; Nakashima, S.; Okada, T. *J. Am. Chem. Soc.* **2002**, *124*, 8398−8405.

(23) Miyasaka, H.; Murakami, M.; Okada, T.; Nagata, Y.; Itaya, A.; Kobatake, S.; Irie, M. *Chem. Phys. Lett.* **2003**, *371*, 40−48.

(24) Miyasaka, H.; Moriyama, T.; Itaya, A. *J. Phys. Chem.* **1996**, *100*, 12609−12615.

(25) Felton, R. H. *The Porphyrins*; Dolphin, D., Ed.; Academic Press: New York, 1978; Vol. V, Chapter 3.

(26) Cadioli, B.; Gallinella, E.; Coulombeau, C.; Jobic, H.; Berthier, G. *J. Phys. Chem.* **1993**, *97*, 7844−7856.

(27) (a) Stein, P.; Ulman, A.; Spiro, T. G. *J. Phys. Chem.* **1984**, *88*, 369−374. (b) Rush, T. S., III; Kozlowski, P. M.; Piffat, C. A.; Kumble, R.; Zgierski, M. Z.; Spiro, T. G. *J. Phys. Chem. B* **2000**, *104* 5020−5034.

(28) Kavarnos, G. J. *Fundamentals of Photoinduced Electron Transfer*; VCH: New York, 1993.

(29) Weller, A. Z. *Phys. Chem.* **1982**, *133*, 93−98.

(30) (a) Asahi, T.; Ohkohchi, M.; Matsusaka, R.; Mataga, N.; Zhang, R. P.; Osuka, A.; Maruyama, K. *J. Am. Chem. Soc.* **1993**, *115*, 5665−5614. (b) Mataga, N.; Chosrowjan, H.; Shibata, Y.; Yoshida, N.; Osuka, A.; Kikuzawa, T.; Okada, T. *J. Am. Chem. Soc.* **2001**, *123*, 12422−12423. (c) Mataga, N.; Chosrowjan, H.; Taniguchi, S.; Shibata, Y.; Yoshida, N.; Osuka, A.; Kikuzawa, T.; Okada, T. *J. Phys. Chem. A* **2002**, *106*, 12191−12201. (d) Yoshida, N.; Ishizuka, T.; Yofu, K.; Murakami, M.; Miyasaka, H.; Okada, T.; Nagata, Y.; Itaya, A.; Cho, H. S.; Kim, D.; Osuka, A. *Chem. Eur. J.* **2003**, *9*, 2854−2866.

(31) DeGraziano, J. M.; Liddell, P. A.; Leggett, L.; Moore, A. L.; Moore, T. A.; Gust, D. *J. Phys. Chem.* **1994**, *98*, 1758−1761.

(32) Sohn, Y. S.; Hendrickson, D. N.; Gray, H. B. *J. Am. Chem. Soc.* **1971**, *93*, 3603−3612.

(33) Bozak, R. E. *Advances in Photochemistry*; Pitts, J. N., Jr., Hammond, G. S., Noyes, W. A., Jr., Eds.; Wiley-Interscience: New York, 1971; Vol. 8, pp 227−244.

(34) Förster, T. *Discuss. Faraday Soc.* **1959**, *27*, 7−17.

(35) Mårtensson, J. *Chem. Phys. Lett.* **1994**, *229*, 449−456.

(36) Kurabayashi, Y.; Kikuchi, K.; Kokubun, H.; Kaizu, Y.; Kobayashi, H. *J. Phys. Chem.* **1984**, *88*, 1308−1310.

(37) Dexter, D. L. *J. Chem. Phys.* **1953**, *21*, 836−850.

(38) Kesti, T.; Tkachenko, N.; Yamada, H.; Imahori, H.; Fukuzumi, S.; Lemmetyinen, H. *Photochem. Photobiol. Sci.* **2003**, *2*, 251−258.

(39) (a) Kilså, K.; Kajanus, J.; Larsson, S.; Macpherson, A. N.; Mårtensson, J.; Albinsson, B. *Chem. Eur. J.* **2001**, *7*, 2122−2133. (b) Pettersson, K.; Kilså, K.; Mårtensson, J.; Albinsson, B. *J. Am. Chem. Soc.* **2004**, *126*, 6710−6719.

(40) Horng, M. L.; Gardecki, J. A.; Papazyan, A.; Maroncelli, M. *J. Phys. Chem.* **1995**, *99*, 17311−17337.

(41) (a) Jean, J. M.; Friesner, R. A.; Fleming, G. R. *J. Chem. Phys.* **1992**, *96*, 5827−5842. (b) Jean, J. M. *J. Phys. Chem. A* **1998**, *102*, 7549−7557.

(42) (a) Wolfseder, B.; Seidner, L.; Domcke, W.; Stock, G.; Seel, M.; Engleitner, S.; Zinth, W. *Chem. Phys.* **1998**, *233*, 323−334. (b) Egorova, D.; Kühl, A.; Domcke, W. *Chem. Phys.* **2001**, *268*, 105−120. (c) Egorova, D.; Domcke, W. *Chem. Phys. Lett.* **2004**, *384*, 157−164.